Meteoritics & Planetary Science 40, Nr 3, 335–342 (2005)
Abstract available online at http://meteoritics.org

The gentle separation of presolar SiC grains from meteorites

J. TIZARD*, I. LYON, and T. HENKEL

University of Manchester, School of Earth, Atmospheric, and Environmental Sciences, Oxford Road, Manchester, M13 9PL, UK
*Corresponding author. E-mail: julia.m.tizard@postgrad.manchester.ac.uk

(Received 8 July 2004; revision accepted 21 January 2004)

Abstract–This paper describes the development of a new, effective, and non-destructive method of SiC isolation from meteorites by freeze-thaw disaggregation, size, and density separation. This new method is important because there is evidence that current methods, which use strong acids and chemical treatments to dissolve silicates and separate out the interstellar grains, may alter the surfaces of the grains chemically and isotopically. Furthermore, any non-refractory coating present on the grains would be destroyed. Using our new separation method, SiC grains were enriched from ~6 ppm abundance in Murchison whole rock to 0.67% abundance in the 0.4–1.4 μm size range and 0.27% abundance in the 1.4–17 μm size range. Individual SiC grains were easily identified using electron probe microanalysis (EPMA) mapping of grains distributed thinly on gold foil; a small aliquot from these fractions has so far yielded >150 SiC grains for isotopic analysis. The method separates out SiC grains efficiently, is applicable to very small or rare samples, and avoids the harsh acid treatments that may alter possible amorphous or non-refractory coats on the grains. The procedure also preserves the remainder of the original sample and it is hoped that it may be extended to other micron-sized presolar grains found in meteorites such as corundum, graphite, and silicon nitride.

INTRODUCTION

Noble gas studies of meteoritic materials in the 1960s (e.g., Reynolds and Turner 1964) revealed large anomalies in isotope signatures, pointing to the survival of presolar materials during solar system formation. Lewis et al. (1987) isolated the first presolar phase, which is diamond. Other presolar phases were isolated soon after: SiC (Bernatowicz et al. 1987), graphite (Amari et al. 1990), silicon nitride (Lee et al. 1992; Nittler et al. 1995), and corundum (Huss et al. 1993). Information on the composition and structure of presolar grains has contributed significantly to our understanding of element synthesis and grain formation in stellar atmospheres and stellar ejecta (Bernatowicz and Zinner 1997; Nittler 2003) and has lead to development in the study of galactic chemical evolution (e.g., Clayton 1997). Presolar grain studies also complement astronomical spectral observations of stars by providing an additional source of information for the physical and chemical conditions within stellar atmospheres and ejecta (Nittler 2003). However, stellar data from spectroscopic observations are limited due to observational constraints. A large proportion of the current information on the physical and chemical conditions in stars has been constrained as a result of comparisons between presolar grain data and theoretical predictions.

Presolar grains comprise only a small fraction of total meteoritic material, varying from several ppb to several hundred ppm in chondritic meteorites. SiC comprises at most 6–8 ppm of a meteorite. Chemical treatment methods that dissolve >99.99% of the bulk meteorite were first developed in the mid-1970s and were refined over the next twenty years (Amari et al. 1994). Variations of this method have been used to isolate almost all SiC grains studied to date. Disadvantages in this method include the loss of less refractory presolar phases (including phases surrounding or intergrown with SiC), abrasion from long total ultrasonication time, and the danger of chemical or isotopic alteration of the grain surface by the harsh acid treatment.

An alternative method for finding presolar grains was published by Bernatowicz et al. (2003), who located 81 presolar SiC grains by extensive and time-consuming SEM X-ray mapping for the 6 ppm of SiC in a disaggregated Murchison whole rock sample. Bernatowicz et al. (2003) found 60% of the SiC grains in their sample to be coated with an apparently amorphous and possibly organic phase. A possible explanation is that grains may have been protected during their residence in the interstellar medium by surface coatings, including simple ices. The composition of these outer layers may hold evidence of the grain's formation and passage through the interstellar medium. Chemical isolation

© The Meteoritical Society, 2005. Printed in USA.

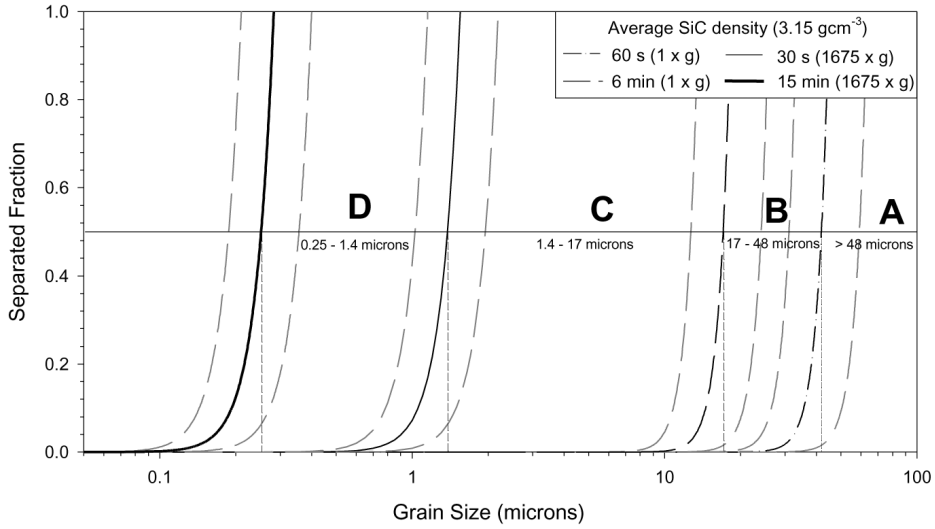

Fig. 1. The fraction of SiC grains of each grain size deposited over four size separations. Resulting grain size separation ranges are taken where >50% (dotted lines) of grains of that size are deposited within the separation time interval. Grey dash-dot lines demonstrate the variation in grain size for grains of density 2 gcm^{-3} and 5 gcm^{-3}.

of SiC, although far more efficient, would most likely remove these amorphous layers, leaving only the refractory core. The desire to isolate SiC grains for single grain analysis efficiently, without harsh acid dissolution techniques, formed the motivation for the process described in this paper.

SiC SEPARATIONS

The Murchison (CM2) meteorite was chosen as the source of SiC grains, as it is a well-characterized carbonaceous chondrite with a high SiC abundance of ~6 ppm. Previous studies of Murchison have identified >99% of SiC as presolar by their anomalous isotopic signatures in SIMS studies (Amari et al. 1994).

Thirty-two mg of Murchison matrix was mined from a fresh cleave of the sample, avoiding visible CAIs and chondrules, then crushed with a stainless steel mortar and pestle and sieved through a 100 μm fine mesh. The fragments were placed in a stainless steel vessel and dispersed in about 1 cm^3 of ultrapure (reverse osmosis) water using a small, non-heated, 45KHz ultrasonic bath. Seventy freeze-thaw cycles, alternately dipping the sample between liquid nitrogen and hot water (~40–60 °C), reduced the matrix fragments to micron-sized grains. Microscopic analysis of 5 individual deposits of the disaggregated sample showed ~70% (by number) of the sample to be in the <10 μm range, with some grains ranging up to 40 μm in size.

Size Separation

The disaggregated sample was suspended in a 1:1 isopropanol-water mixture. The grains were distributed over the full length of the tube by agitation for 5 min in the ultrasonic bath. A size separation timetable was calculated from Stokes' law:

$$SR = \left(\frac{gd^2\rho_g - \rho_s}{18v_s}\right) \quad (1)$$

Sedimentation rates *SR* were calculated for average SiC density (3.15 gcm^{-3}). The viscosity v_s of the isopropanol-water mixture was taken to be 0.0038 Nsm^{-2} (at 20 °C) and the density ρ_s to be 0.85 gcm^{-3}. The viscosity of isopropanol in particular varies significantly with temperature. Sedimentation rates range within 10–20% for a 5–10 degree temperature change. Sedimentation times were calculated for the full length of the tube (4 cm), ensuring that 100% of the grains within a chosen size range would have time to sediment. Because smaller grains nearer the bottom of the tube sediment in the same time as larger grains at the top, repeat separations were made at each interval to sharpen the size separation boundaries.

Sedimentation rates for smaller grains (<10 μm) were impractically long, so a centrifuge was employed to speed up the process. The use of a fixed angle rotor centrifuge causes some deviation from Stokes' law sedimentation, as particles are pushed toward the outer walls of the centrifuge tubes and may sediment in bulk with other particles. This may cause smaller grains to sediment faster than Stokes' law calculations. Multiple repetitions of the size separation steps and the distribution of the sample over the length of the tube should go some way in combating this effect.

SiC size fractions were chosen as: A > 48 μm, B = 17–48 μm, C = 1.4–17 μm, and D = 0.25–1.4 μm by the corresponding time intervals and g-forces of 60 sec (at 1 g), 6 min (at 1 g), 30 sec (at 1675 g), and 15 min (at 1675 g).

Table 1. Details of the organic heavy liquids from Cargille Laboratories used to perform the density separations.

Cat N°	Density (gcm^{-3})	Viscosity (Nms^{-2})
12440	2.95	0.00147
12460	3.05	0.00305
12470	3.14	0.00314
12480	3.19	0.00638
12490	3.24	0.00648

Table 2. Details of the various density separation steps for the D and C size separation fractions. The resultant density ranges in the D samples (see Fig. 2) meant higher separations were not needed.

Density separation (gcm^{-3})	Size separation (microns)	G-force (g)	Time interval (min)
2.95	1.4–17	3287	6
3.05	1.4–17	3287	12
3.14	1.4–17	3287	12
3.19	1.4–17	3287	25
3.24	1.4–17	3287	25
2.95	0.25–1.4	4290	25
3.05	0.25–1.4	4290	30
3.14	0.25–1.4	4290	30

Starting with the largest size separation, the substrate and suspended grains were siphoned from the tube at the end of each time interval, leaving only the sedimented grains. The size separation was repeated for both the sediment and suspended samples. The A and B size fractions were repeated five times each. The C and D size separations were repeated three times. After repeat separations, all the sediments from the same size separation step were added and the suspensions similarly accumulated. Each sample was redistributed over the entire length of the tube by agitating for 5 min in the ultrasonic bath prior to each repeat separation in order to discourage the clumping of grains. Through the repeat separation process the sample size for each separation was split in two, thus, the separations are clarified with each repetition. Each size-separated sample was dried before proceeding to the next separation.

The fraction F of grains of specific size deposited by Stokes' law in a given time t is given in Equation 2, where h is the height of the separation tube and n the number of repeat separations. Figure 1 demonstrates the calculated separation fractions for grains of SiC density.

$$F = \left(\frac{SR \cdot t}{h}\right)^n \quad (2)$$

The times for the final size separation (band D) were chosen for grains with a lower size limit of 0.25 μm. However, this does not define the size cutoff for this group, as a final 10 min of centrifugation at 4000 × g was carried out at the end of the separation process to deposit the smallest grains.

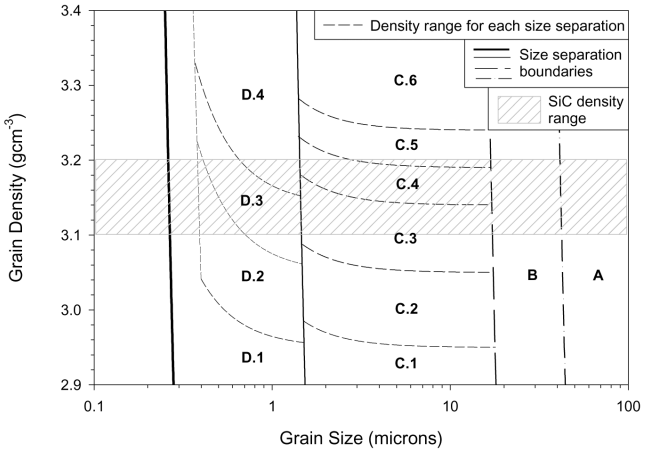

Fig. 2. Resulting size and density bands from the series of separations. Dashed lines depict the boundaries between density separations based on depositing >50% of the grain size within three repeat density separations.

Density Separation

To isolate SiC grains from other minerals, separation by density was used. The known density of SiC ranges from 3.1 gcm^{-3} to 3.2 gcm^{-3}, depending on the crystalline structure of the mineral. Studies (Bernatowicz et al. 2003; Daulton et al. 2002, 2003) have found presolar SiC in only two polytypes, the cubic 3C (beta-SiC) polytype (~80% by number) and the hexagonal 2H (alpha-SiC) polytype (~3%) with the remainder forming intergrowths of the two or disordered structures. Since the cubic crystalline structure is the most compact formation of the polytype structures, we would expect presolar SiC to fall into the higher end of the SiC density range.

A series of organic heavy liquids (Cargille Laboratories) was used to perform the density separations (see Table 1). The heavy liquids were chosen for their low viscosity, chemical stability, and density range for SiC isolation. The organic heavy liquid range is known to degrade with exposure to sunlight. Exposure to light was minimized by careful storage of the liquids in the dark and by covering the sample tubes with foil during the separation procedure. Test amounts of heavy liquid exposed to sunlight showed significant degradation only after 10 hr.

Starting with the lowest density first, heavy liquid was introduced to the different size separations and mixed thoroughly by agitation for 10 and 25 min in an ultrasonic bath for the C and D separations, respectively. Each sample was then centrifuged using a fixed angle rotor centrifuge according to a specific timetable, calculated from Stokes' law:

$$t = \left(\frac{18hv_s}{gd^2(\rho_g - \rho_s)}\right) \quad (3)$$

Small grains are harder to sediment from the heavy liquid than larger grains, requiring longer separation times

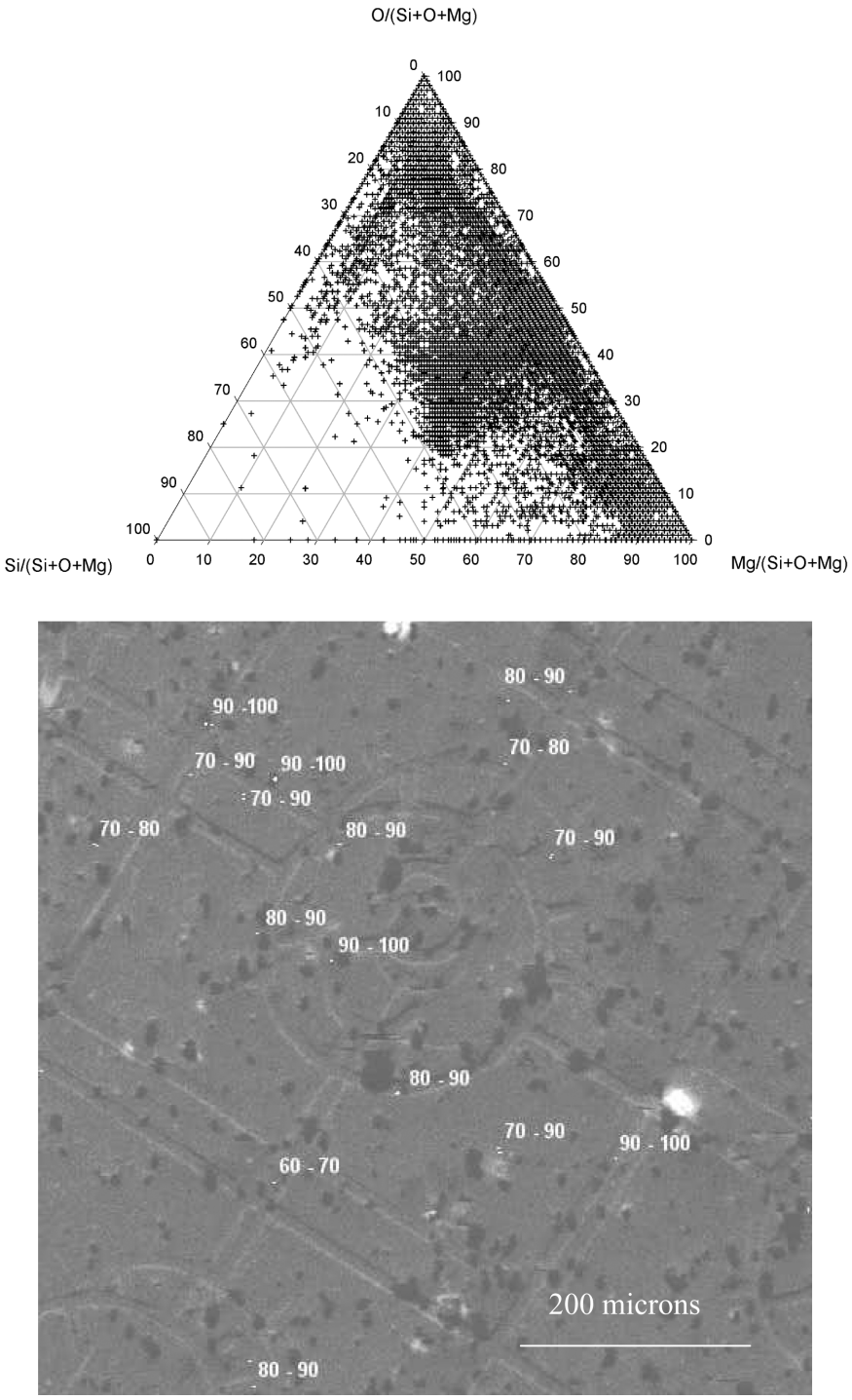

Fig. 3. a) Ternary plot of processed EPMA data of one area (512 × 512 μm) from the C.3 sample. SiC candidate grains are clearly visible as the small group above ~60% Si/(Si + O + Mg). Each cross may represent more than one grain. b) Pixel-by-pixel map of the Si/(Si + O + Mg) ratios of the C.3 candidate grains and detail of their location with reference to an imprinted grid.

and larger g-forces. Hence, a spread in the density of grains sedimented will be produced from the spread in the size range of the grains in each density separation step of liquid density ρ*s*, time interval *t*, and g-force *g*. In a single density step, small grains will have higher density than the larger grains, effectively introducing a secondary size separation. Similar to the case of the size separations, the use of the fixed angle rotor centrifuge will cause some deviation from Stokes' law sedimentation, allowing some portion of smaller grains to sediment faster. This is expected to lessen the effect

of the secondary size separation. It is not expected to significantly alter the density cutoff in each separation, as grains with lower density than the heavy liquid should stay in suspension.

The separation times and g-forces (Table 2) were chosen to reflect a good density separation across all grain sizes in the size separation range (Fig. 2). The A and B size fractions were not density-separated, as the abundance of SiC >10 μm in size is extremely low (Amari et al. 1994).

After each separation, the supernatant suspension was withdrawn, leaving only the sedimented sample. Both the sediment and floating separation were washed repeatedly in acetone (a solvent was required to dilute the heavy liquid) and then in pure water. The density separation was then repeated, with washes, for both the sediment and the floating separations a minimum of three times per separation before moving on to the next density separation step. The samples were agitated in the ultrasonic bath for 10 min during the rinsing stage to ensure good extraction of the heavy liquid and again for 10 min before the next separation step to mix the sample thoroughly with the heavy liquid and encourage amassed particles to detach, respectively.

Figure 2 shows the Stokes' law calculations for the entire separation process and details in which fractions SiC grains of specific size and density are expected to be located.

The upper limit of the centrifuge (4290 g when using heavy liquids) was not able to sediment grains below ~0.4 μm from the lightest heavy liquid density step (2.95 gcm^{-3}). These grains were not lost, as they were sedimented from diluted heavy liquid washes following the 2.95 gcm^{-3} separation. However, they were consequently not separated by density and remain in the D.1 separation (see Fig. 2).

Other Factors Affecting the Separation Process

Non-Stokes' law effects, such as surface tension and Brownian motion on very small grains, may slow or halt the sedimentation of grains. This may cause small grains to appear in a lower density separation band and may generally cause overlap in the separation boundaries. These two effects are dependant on both the viscosity of the heavy liquid and the size of the grains. They are therefore more prevalent in both the higher density separations and the smaller grain size separations. The choice of low viscosity heavy liquids, the use of the ultrasonic bath for mixing, and the use of the centrifuge to encourage deposition and repetition of each separation should minimize these effects as a source of error in isolating and locating SiC grains.

A larger uncertainty affecting the calculated separation times of the grains is expected from the inherent assumption of spherical grains in Stokes' law. Density averaging may also affect the location of SiC within the size density separations. Coatings around the SiC grains may give the grains an average density lower or higher than the expected SiC density of 3.1 gcm^{-3} to 3.2 gcm^{-3}.

Heavy Liquid Contamination Issues

Contamination of the grains by elements in the heavy liquids is clearly a concern for element and isotope analysis. The composition of each heavy liquid used was therefore analyzed by inductively coupled plasma mass spectrometer (VG Elemental Plasmaquad 2 STE) for potential contamination problems. Most elements showed an abundance of less than 2 ppb. Na (110–340 ppb), Cu (40–120 ppb), Se (15–310 ppb), and Zn (350 ppb in the lower density fraction) were the only elements to have over 100 ppb concentrations. Of the larger contributions, Na is mono-isotopic and therefore of little interest in isotope studies. The high abundance of Zn may be due to its use as a catalyst in the manufacture of halogenated hydrocarbons, which form the base of the heavy liquid composition. Cu and Se have not been of interest to date in presolar meteoritic material studies. Furthermore, a rigorous washing regime was added to the separation process to reduce the risk of any contamination of the samples from the heavy liquids used.

EXPERIMENTAL PROCEDURE: SiC GRAIN LOCATION

SiC was located in the enriched separates by electron probe mapping of the grains for Si, C, Mg, and O. A 5 × 5 mm piece of high purity gold foil was imprinted with an Agar, H15, 3.05 mm, 125 mesh, Copper Finder-Grid to leave an impression in the gold of the grid wires and location symbols. A small aliquot of each of the D.2 and D.3 and C.2, C.3, and C.4 samples, suspended in a 1:1 isopropanol-water mixture, was then spread over the prepared foils.

A total area of 1.8 mm^2 of each of these samples was mapped in six 512 × 512 pixel images with a Cameca SX100 electron microprobe (EPMA), using an approximate beam diameter of 1 μm. SiC grain candidates were identified from Si/(Si + O + Mg) count ratios of those individual pixels with counts above a background threshold of 10 counts (sample C) or 5 counts (sample D).

Figures 3a and 3b show examples of the processed EPMA data of one area from the C3 sample. The Fig. 3a ternary plot clearly highlights the presence of SiC candidates and Fig. 3b shows the position of the candidate grains superimposed onto an EPMA map of the area in carbon, which details their location with reference to the imprinted grid.

RESULTS

Effective Size and Density Separations

The semi-major and semi-minor axes of 200 grains of a range of mineralogies across 12 randomly chosen areas of the C and D samples were measured to judge the quality of the size separations. This was done using high spatial resolution

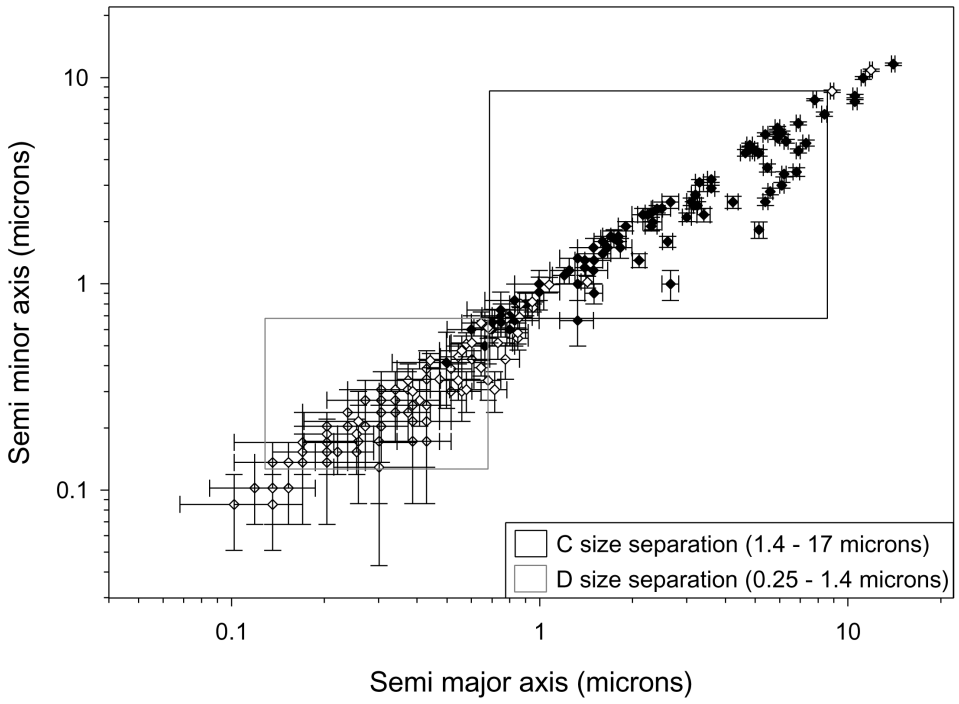

Fig. 4. Size distributions within the C (filled symbols) and D (open symbols) samples. The semi-major and semi-minor axes of 200 grains from 12 randomly chosen areas on the C and D samples are shown. Measurements were taken by SEM imaging of individual grains. Errors shown in the figure represent the accuracy to which the grains could be measured from the images, depending upon the pixel size of the image.

SEM images with varying magnification. Figure 4 shows the resulting distribution of grain size and symmetry across the two separations.

The majority of grains lie within the calculated size separation boundaries. 10% of the C separation and 18% of the D separation lie outside their calculated size range. This is expected, as calculations for the time scales of the separations were based on Stokes' law sedimentation for 50% of the grains in each size range. Some deviation from Stokes' law was expected due to the use of the fixed angle rotor centrifuge (see Size Separation section). This may account for the overlap of smaller grains in the larger C size separation and the presence of grains smaller than 0.25 μm in the D size separation. Grains sizes below 0.4 microns also push the limit of the SEM spatial resolution and as such probably warrant larger error.

It is thought that other non-Stokes' law effects such as asymmetric grain shape (see Other Factors Affecting the Separation Process section) may be a dominant factor contributing to the presence of grains in the smaller size separation that are larger than expected. There is also the possibility of cross-contamination between the suspension and sediment in each size separation as the suspension is extracted; the last remains of the suspension are in close contact with the sedimented sample and thus some pickup of the sediment may be expected during this removal process. In order to avoid pickup from the sedimented sample, only 95% of the suspension was removed from the tube after each separation. This may account for the two grains, ~9 and 11 microns, in the D sample that are an order of magnitude larger in size than expected for the D size separation.

Overall, Fig. 4 shows a good correlation between the actual size range of grains and the calculated range, with >84% of grains conforming to the desired size separation bands.

SiC Isolation

Accuracy of the density separations can be determined by the efficiency of SiC isolation. The D.3, C.3, and C.4 samples were studied to locate and verify the presence of SiC and the D.4, C.2, and C.5 samples were studied to determine the extent of isolation of SiC and the accuracy of the density separations.

D.3, C.3, and C.4 Samples

From an initial 32 mg sample of Murchison matrix, ~0.2 mg, ~0.8 mg, and ~0.5 mg were separated into the D.3, C.3, and C.4 fractions, respectively. 120 SiC grains were identified in a 1.8 mm^2 area of a small aliquot of the D.3 separation spread over gold foil. Each of these grains was verified to be SiC by EDS analysis of the SiC candidate grains identified from EPMA mapping. The success rate for verified SiC from the candidate grains was 80% for the D.3 sample.

22 and 14 grains were also located within a 1.8 mm^2 area on the C.3 and C.4 samples, respectively. Verification of candidate grains by EDS analysis in the C.3 and C.4 samples

revealed a success rate of ~60% in accurately locating SiC in the C.3 and C.4 separations by EPMA mapping. The reason for the reduced accuracy in EMPA identification of SiC grains was due in part to charging effects of the larger grains during EPMA mapping. Charging of the larger grains leads to the local defocusing of the electron probe beam and consequently to the averaging of signals from neighboring grains. Heterogeneity between elements, on order of 1–2 μm in larger grains, also contributed to the misidentification of SiC grains.

It was noted during EDS verification of the composition of the candidate grains that only about 10% of the "false" (non-SiC) candidate grains were Mg and/or O composites. The majority of the false candidates were rich in Fe or Al in addition to being rich in Si. Adding Fe and/or Al to the elements mapped with the EPMA could thus improve the accuracy of detecting SiC with this method.

The average spread of grains over the gold foils of these samples was ~9900 grains per mm^2 for D.3, ~3800 grains per mm^2 for C.3, and ~3500 grains per mm^2 for the C.4 sample, resulting in an increase of the abundance of SiC in these fractions from ~6 ppm to 0.67%, 0.32%, and 0.22%, respectively. When compared to 0.32% in the larger size fraction, 0.67% is lower than expected when the Murchison SiC size distribution is taken into account. However, the beam diameter for the EPMA mapping, which is about 1 μm, may lower the efficiency for detecting grains below 1 μm in size.

D.4, C.2, and C.5 Samples

The D.4, C.2, and C.5 samples were put through the same EPMA mapping and EDS postanalysis of candidate grains in order to determine the extent of SiC isolation. Samples were mapped over a 1.8 mm^2 area. The average spread of grains over these samples was similar to that of the C.3 and C.4 samples.

No SiC grains were found in any of the sample deposits. SiC candidates were observed in the EPMA mapping; however, EDS postanalysis of these candidate grains revealed silicates only. The majority of the false grains were found to be rich in Ca, Fe, or Al or were due to charging effects, similar to misidentified grains in the previous samples.

SUMMARY

From an initial 32 mg sample of Murchison whole matrix, ~0.2 mg, ~0.8 mg, and ~0.5 mg were separated into the 0.4–1.4 μm (D.3) and 1.4–17 μm (C.3 and C.4) size fractions covering the SiC density range. 120, 22, and 14 SiC grains were located within 1.8 mm^2 area deposits from a small aliquot of these fractions, respectively. No SiC grains were found in higher or lower density fractions of these size ranges (D.4, C.2, and C.5). Overall, SiC grains were enriched from ~6 ppm abundance in Murchison whole rock to 0.67% abundance in the 0.4–1.4 μm, SiC density range (D.3) fraction and 0.32% and 0.22% in the 1.4–17 μm SiC density range (C.3 and C.4, respectively).

The increase in abundance of SiC from 6 ppm to percent levels across the expected SiC isolation bands and the lack of SiC identified within higher and lower density separations demonstrates the efficiency of the density separation procedure on even very small meteorite samples. The grains are identified in known locations on a gold grid, allowing subsequent single-grain probe analyses for morphology, element, or isotopic compositions. The separation method also retains all other minerals in the meteorite whole matrix.

It is hoped that gentle separation protects the chemical and physical characteristics of the grains, particularly any external coatings that the grains may have acquired through their travels in the ISM and solar nebula. Further work on this separation method, and in particular on the extension of the heavy liquid density range, is also hoped to open the method to the isolation of other meteorite fractions of interest.

ACKNOWLEDGEMENTS

We thank D. Plant and S. Caldwell for their technical support in the analysis of data on the Electron Probe & Environmental SEM. We also thank P. Lythgoe for assistance in obtaining the ICPMS data on the composition of the heavy liquids. G. Turner is appreciated for encouragement and discussion of this work, as are R. Lewis, S. Verchovsky, and an anonymous reviewer for his or her constructive reviews. PPARC is acknowledged for support of this work through a studentship to JMT and research position to TH.

Editorial Handling—Dr. Ian Franchi

REFERENCES

Amari S., Anders E., Virag A., and Zinner E. 1990. Interstellar graphite in meteorites. *Nature* 345:238–240.

Amari S., Lewis R. S., and Anders E. 1994. Interstellar grains in meteorites. I. Isolation of SiC, graphite, and diamond: Size distributions of SiC and graphite. *Geochimica et Cosmochimica Acta* 58:459–470.

Bernatowicz T. J. and Zinner E., eds. 1997. *Astrophysical implications of the laboratory study of presolar materials*. New York: American Institute of Physics. 778 p.

Bernatowicz T. J., Fraundorf G., Tang M., Anders E., Wopenka B., Zinner E., and Fraundorf P. 1987. Evidence for interstellar SiC in the Murray carbonaceous meteorite. *Nature* 330:728–730.

Bernatowicz T. J., Messenger S., Pravdivtseva O., Swan P., and Walker R. M. 2003. Pristine presolar silicon carbide. *Geochimica et Cosmochimica Acta* 67:4679–4691.

Clayton D. D. 1997. Placing the sun and mainstream SiC particles in galactic chemodynamic evolution. *The Astrophysical Journal* 484:L67–L70.

Daulton T. L., Bernatowicz T. J., Lewis R. S., Messenger S., Stadermann F. J., and Amari S. 2002. Polytype distribution in circumsteller silicon carbide. *Science* 296:1852–1855.

Daulton T. L., Bernatowicz T. J., Lewis R. S., Messenger S.,

Stadermann F. J., and Amari S. 2003. Polytype distribution of circumstellar silicon carbide: Microstructural characterization by transmission electron microscopy. *Geochimica et Cosmochimica Acta* 67:4743–4767.

Huss G. R., Hutcheon I. D., Fahey A. J., and Wasserburg G. J. 1993. Oxygen isotope anomalies in Orgueil corundum: Confirmation of presolar origin (abstract). *Meteoritics* 28:369.

Lee M. R., Russel S. S., Arden J. W., and Pillinger C. T. 1992. The isotopic composition and mineralogy of silicon nitride (Si_3N_4) within ordinary and enstatite chondrites (abstract). *Meteoritics* 27:248–249.

Lewis R. S., Tang M., Wacker J. F., Anders E., and Steel E. 1987. Interstellar diamonds in meteorites. *Nature* 326:160–162.

Nittler L. R. 2003. Presolar stardust in meteorites: Recent advances and scientific frontiers. *Earth and Planetary Science Letters* 209: 259–273.

Nittler L. R., Hoppe P., Alexander C. M. O. D., Amari S., Eberhardt P., Gao X., Lewis R. S., Strebel R., Walker R. M., and Zinner E. 1995. Silicon nitride from supernovae. *The Astrophysical Journal* 453:L25–L28.

Reynolds J. H. and Turner G. 1964. Rare gases in the chondrite Renazzo (abstract). *Journal of Geophysical Research* 69:3263.